# Chiral and deconfinement phase transitions of two-flavour QCD at finite temperature and chemical potential

Christian S. Fischer,[1,2] Jan Luecker,[1] and Jens A. Mueller[3]

[1] Institut für Theoretische Physik, Justus-Liebig-Universität Gießen, Heinrich-Buff-Ring 16, D-35392 Gießen, Germany

[2] GSI Helmholtzzentrum für Schwerionenforschung GmbH, Planckstr. 1 D-64291 Darmstadt, Germany.

[3] Institut für Kernphysik, Technische Universität Darmstadt, Schlossgartenstraße 9, D-64289 Darmstadt, Germany

(Dated: January 19, 2013)

We present results for the chiral and deconfinement transition of two flavor QCD at finite temperature and chemical potential. To this end we study the quark condensate and its dual, the dressed Polyakov loop, with functional methods using a set of Dyson-Schwinger equations. The quark-propagator is determined self-consistently within a truncation scheme including temperature and in-medium effects of the gluon propagator. For the chiral transition we find a crossover turning into a first order transition at a critical endpoint at large quark chemical potential, $\mu_{EP}/T_{EP} \approx 3$. For the deconfinement transition we find a pseudo-critical temperature above the chiral transition in the crossover region but coinciding transition temperatures close to the critical endpoint.

**Introduction**

Heavy ion collision experiments at RHIC, the LHC and the future FAIR project are designed to study the properties of the large temperature phase of QCD, the quark-gluon plasma. Of particular interest are the details of the chiral and deconfinement transition. Here, a standard scenario favors a chiral crossover at small chemical potential turning into a first order chiral transition at a critical point. The search for this critical point is one of the main motivations in the physics program of the future CBM/FAIR experiment in Darmstadt and the NICA project in Dubna. However, on the theoretical side there is ambiguity not only about the location of the critical point but also if the standard scenario is even correct. Among other possibilities [1] an exotic, quarkyonic matter phase [2] or inhomogeneous chiral condensates [3, 4] could be realized. Unfortunately, lattice Monte-Carlo simulations cannot be used to resolve this issue due to the notorious sign problem.

Effective models to QCD like the Polyakov-loop extended Nambu–Jona-Lasinio model (PNJL) [5] and the Polyakov-loop extended quark-meson model (PQM) [6, 7] constitute an alternative approach. Much progress has been made taking into account fluctuations beyond mean-field [7], which shift for example the critical endpoint to larger chemical potential. Interestingly this is in agreement with recent lattice results indicating that the critical endpoint if existent is at much larger chemical potential [8] than previously thought [9].

Within QCD fortunately also non-perturbative tools not limited by the sign problem are at our disposal. In particular, it has been shown that Dyson-Schwinger equations (DSEs) and the functional renormalization group [10–16] are capable to describe both, the chiral and the deconfinement transition at finite temperatures and imaginary chemical potential [12, 14].

In this letter we extend these applications to finite, real chemical potential. We use the DSEs for the propagators of Landau gauge QCD with two fermion flavors in a suitable truncation scheme. Working with physical quark masses we determine the quark condensate and its dual, the dressed Polyakov loop in the real $(T, \mu)$-plane. We extract transition temperatures for the chiral and deconfinement transition and determine their nature. We locate the critical endpoint of the chiral transition. Our study provides the tools for further, more detailed investigations of gauge invariant properties of the QCD phase diagram by functional methods.

**Order parameters**

We calculate the order parameters for chiral symmetry breaking and confinement from the fully dressed quark propagator, given by

$$S^{-1}(p) = i\vec{\gamma}\vec{p}A(p) + i\gamma_4(\omega_n + i\mu)C(p) + B(p), \quad (1)$$

where $\mu$ is the quark chemical potential and $\omega_n = \pi T(2n+1)$ are the Matsubara modes in the imaginary time formalism with temperature $T$. The argument $(p)$ serves as an abbreviation for $(\vec{p}^2, \omega_n)$. The scalar and vector dressing functions $B$ and $A, C$ are calculated from the quark DSE. For the bare, renormalized propagator $S_0^{-1}(p)$ we have $A = C = Z_2$ and $B = m$, where $m$ is the renormalized bare quark mass and $Z_2$ is the quark renormalization factor.

There are several equivalent choices of order parameters for chiral symmetry breaking; here we use

the quark condensate

$$\langle\bar{\psi}\psi\rangle = Z_2 T \sum_n \int \frac{d^3p}{(2\pi)^3} \mathrm{Tr}_D\left[S(p)\right]. \qquad (2)$$

We work with two degenerate quark flavors with physical quark masses and therefore expect a smooth crossover at vanishing chemical potential [9]. Below, we determine the transition temperatures via the maximum of the susceptibility $\frac{\partial\langle\bar{\psi}\psi\rangle}{\partial m}$.

Extracting an order parameter for confinement from the quark propagator is a much more challenging task. In the last years a method has been developed to calculate dual condensates $\Sigma_n$ which are sensitive to centre symmetry breaking [17–19]. They are defined by the transform

$$\Sigma_n = \int_\varphi e^{-i\varphi n}\langle\bar{\psi}\psi\rangle_\varphi, \qquad (3)$$

where $\int_\varphi \equiv \int_0^{2\pi}\frac{d\varphi}{2\pi}$ and $\langle\bar{\psi}\psi\rangle_\varphi$ is the quark condensate evaluated at generalized, $U(1)$-valued boundary conditions $\psi(\vec{x},1/T) = e^{i\varphi}\psi(\vec{x},0)$ with $\varphi \in [0,2\pi[$. On a lattice, the quantity $\Sigma_n$ can be interpreted as a sum of all closed loops winding $n$ times around the Euclidean time direction. Consequently, $\Sigma_{+1}$ contains the Polyakov loop and $\Sigma_{-1}$ its conjugate, together with all other oriented loops that wind once around the space-time torus. They therefore have been called 'dressed Polyakov loop' and its conjugate [19]. For $\Sigma_{\pm1}$ to act as order parameters for deconfinement it is mandatory to implement the generalized, $U(1)$-valued boundary conditions only on the level of observables, but not in the partition function itself. All closed quark loops therefore maintain the physical value $\varphi = \pi$, whereas $\varphi \in [0,2\pi[$ for the test quark in Eq. (3). This procedure breaks the Roberge-Weiss symmetry, a necessary condition for the dual condensate to act as an order parameter for centre symmetry breaking [14, 20].

For our choice of physical quark mass we expect a deconfinement crossover at small $\mu$. To determine the pseudo-critical temperature we use the maximum of the derivative with respect to the quark mass.

**Dyson-Schwinger equations**

The quark propagator is calculated from its Dyson-Schwinger equation (DSE), shown in the first line of Fig. 1. It depends on the dressed quark-gluon vertex and the dressed gluon propagator, which need to be specified. For the Landau gauge gluon propagator at finite temperature, the most reliable source up to now are quenched lattice calculations [13, 21]. Since we are interested in studying the transition temperatures and the nature of the transitions at non-vanishing chemical potential it is mandatory to include quark in-medium effects in the gluon propagator. To this end we use the lattice data from Ref. [13] for the quenched gluon and add the quark polarization tensor from the gluon DSE to effectively unquench the system, see second line of Fig. 1. This procedure is not entirely selfconsistent. In particular unquenching effects in the Yang-Mills part of the gluon-DSE, i.e. in the ghost-loop and gluon-loop diagrams hidden in the quenched gluon in Fig. 1 are neglected. In the vacuum we compared these effects with the fully selfconsistent treatment of Ref. [22]. We found that the approximation used here overestimates the unquenching effects, with momentum dependent deviations in the gluon propagator below the five percent level. Assuming that this remains so at finite temperature and chemical potential one would expect to slightly underestimate the transition temperatures perhaps on the 5-10 MeV level. We believe that such a treatment is sufficiently accurate for the qualitative study envisaged in this work.

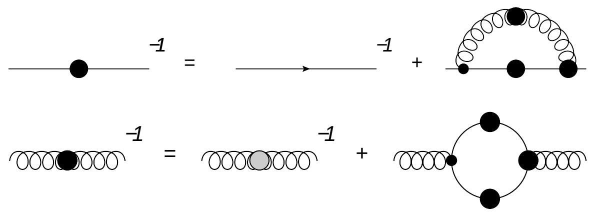

FIG. 1: The DSE for the quark and gluon propagators. Filled circles denote dressed propagators and vertices. The shaded circle denotes the quenched gluon.

Within the polarization tensor we additionally neglect the quark self-energies in analogy with corresponding works on finite density-QCD in the DSE formalism [23]. This approximation is justified by findings comparing lattice and DSE results for the quark spectral function [15] showing that the self-energies are suppressed close to the transition temperature. The tensor is then given by

$$\Pi_{\mu\nu}(p) = \frac{Z_{1F}N_f}{2} \sum\!\!\!\!\!\!\!\int_k \mathrm{Tr}\left[S_0(q)\gamma_\mu S_0(k)\Gamma^0_\nu\right], \quad (4)$$

with $q = p + k$, $\sum\!\!\!\!\!\!\int_k \equiv \sum_n \int \frac{d^3k}{(2\pi)^3}$, the vertex renormalization $Z_{1F}$ and the quark-gluon vertex for bare propagators $\Gamma^0_\nu(p) = g\gamma_\nu\Gamma(p)$, discussed below.

Projected to modes longitudinal (L) and transversal (T) to the medium, the gluon DSE reads

$$\left(Z_{T,L}(p)\right)^{-1} = \left(Z^{qu.}_{T,L}(p)\right)^{-1} + \Pi_{T,L}(p), \qquad (5)$$

with the quenched and unquenched gluon dressing functions $Z^{qu.}_{T,L}$ and $Z_{T,L}$, respectively, and the quark loop $\Pi_{T,L}$. Equation (5) may be evaluated in leading order hard thermal loop where we obtain thermal momentum dependent masses

$$m^2_{T,L}(p) = \frac{N_f\,\pi\,\alpha_{T,L}(p)}{3}\left(T^2 + \frac{3\mu^2}{\pi^2}\right) \quad (6)$$

with $\alpha_{T,L}(p) = Z_{1F}g^2 Z_{T,L}(p)\Gamma^0(p)/(Z_2^2\,4\pi)$.

For the quark-gluon vertex $\Gamma_\nu$ at finite temperature no information is available yet, neither from the lattice nor from functional methods. For the purpose of this study we therefore rely on a phenomenological *ansatz* that has been developed in earlier works, Ref. [12, 13]. To make this work self-contained we repeat the vertex here,

$$\Gamma_\nu(q,k,p) \;=\; \widetilde{Z}_3\left(\delta_{4\nu}\gamma_4\frac{C(k)+C(p)}{2}+\delta_{j\nu}\gamma_j\frac{A(k)+A(p)}{2}\right)\left(\frac{d_1}{d_2+q^2}+\frac{q^2}{\Lambda^2+q^2}\left(\frac{\beta_0\alpha(\mu)\ln[q^2/\Lambda^2+1]}{4\pi}\right)^{2\delta}\right) \quad (7)$$

where $q = (\vec{q},\omega_q)$ denotes the gluon momentum and $p = (\vec{p},\omega_p)$, $k = (\vec{k},\omega_k)$ the quark and anti-quark momenta, respectively. Furthermore $2\delta = -18N_c/(44N_c - 8N_f)$ is the anomalous dimension of the vertex. This ansatz contains the quark dressing functions $A$ and $C$ in a manner dictated by the Slavnov-Taylor identity of the vertex. It therefore implicitly depends on temperature and chemical potential in a meaningful way and also contains unquenching effects via the corresponding changes in $A$ and $C$. In the quark-DSE we keep this dependence, whereas in the gluon polarization we set $A = C = 1$ to be consistent with the HTL approximation described above.

The parameters $d_1$,$d_2$ and $\Lambda$ of the vertex have been fixed in Ref. [13] for the case of quenched QCD. The temperature independent scale $\Lambda$ is associated with the scale of the lattice data for the gluon propagator and given by $\Lambda = 1.4$ GeV. The parameter $d_2$ is associated with the transition from the logarithmic ultraviolet running of the vertex towards the infrared constant and is given by $d_2 = 0.5\,\mathrm{GeV}^2$. Moreover, $d_1 = 4.6\,\mathrm{GeV}^2$ parametrizes the infrared strength of the vertex. Both, $d_1$ and $d_2$ have been fixed in Ref. [13] such that the chiral and deconfinement transition temperatures extracted from the quenched quark propagator matched the deconfinement transition temperature taken from the Yang-Mills lattice input. Note that this procedure is not very sensitive, i.e. it does not require any fine-tuning: once $d_1$ and $d_2$ are in the right ballpark, the resulting transition temperatures have been found to be insensitive to variations of $d_1$ and $d_2$ up to the ten percent level. Thus once the vertex is chosen such that it roughly matches the lattice gluon propagator, its details are not so relevant. This is certainly reassuring. Using a bare quark mass of $m(\mu = 30\,\mathrm{GeV}) = 3.7$ MeV we also determined the resulting (quenched) pion mass at zero temperature, which is roughly ten percent above its physical value and independent of changes in $d_1$ and $d_2$.

In our unquenched calculation we use the same vertex parameters as in the quenched case. This choice is only justified by simplicity. In general, one also expects unquenching effects in the vertex, which may affect the transition temperatures. One way to determine the corresponding changes in $d_1$ and $d_2$ would be to calculate unquenched observable like the pion mass and decay constant in the $T = 0$ limit and match to experiment. Unfortunately this cannot be done within the HTL approximation of the quark polarization used in this work, since it only contains temperature dependent fluctuations which vanish in the $T = 0$ limit. A more refined treatment of the quark backreaction including also quantum fluctuations is under way and will be presented in a future work. We do, however, not expect that unquenching effects in the vertex will have a large impact on the transition temperatures. At zero temperature and with fixed gluon propagator these effects have been found to reduce light hadron masses on the ten percent level [24]. Thus with fixed gluon propagator one may expect that unquenching effects in the vertex will reduce the transition temperatures by a similar amount. This is, however, counterbalanced by a corresponding decrease of quark polarization effects in the gluon propagator, which in turn increases the transition temperatures again. Thus the combined effect may indeed be very small.

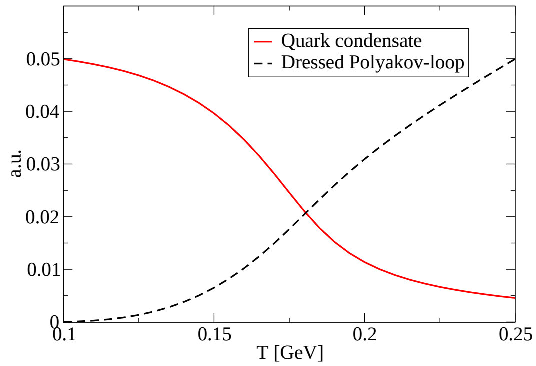


FIG. 2: The quark condensate as well as the dressed Polyakov-loop as a function of temperature in two-flavour QCD.

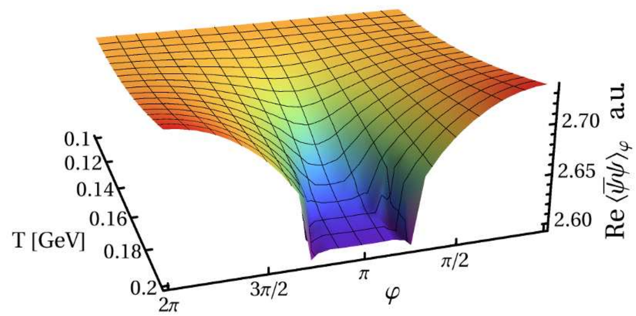


FIG. 3: The quark condensate $\langle\bar{\psi}\psi\rangle_\varphi$ as a function of temperature and boundary angle $\varphi$ at fixed quark chemical potential $\mu = 100$ MeV.

**Results**

As a first check of the employed truncation scheme we determine the transition temperatures at $\mu = 0$. In the quenched system, i.e. without the quark-loop contribution of Eq. (4), our system of equations reduces to the one outlined in Ref. [13] and we obtain $T_c^{N_f=0} = T_{deconf}^{N_f=0} = 277$ MeV. This is in accordance with lattice caluclations. When we switch from $N_f = 0$ to $N_f = 2$ the main effect of the quark loop onto the gluon propagator is to decrease its strength and to lower the characteristic scale $\Lambda_{QCD}$. This also results in decreased chiral and deconfinement transition temperatures. We obtain $T_c^{N_f=2} = 180 \pm 5$MeV and $T_{deconf}^{N_f=2} = 195 \pm 5$MeV which is again close to the corresponding values on the lattice [25]. Here the error bar reflects possible numerical uncertainties in our calculation. The additional sources for systematic errors of our calculation have been discussed in the last section. As a rough guidance for the reader we guesstimate an additional systematic error of $\pm 20$MeV.

Our results for the quark condensate and the dressed Polyakov-loop are shown in Fig. 2. In the quenched calculation of Ref. [13] a sharp rise and fall of the quark condensate close to $T_c$ has been observed, which has been attributed to a corresponding behavior of the electric part of the gluon propagator. Here, the backreaction of the quark-loop has suppressed this effect and the condensate decreases monotonically as expected. This change of behavior together with the correct order of the transition temperatures gives us confidence, that our implementation of the backreaction of the quarks onto the Yang-Mills sector serves its purpose.

We then switch on the chemical potential and determine the chiral condensate as well as the dressed and the conjugate dressed Polyakov loop in the $(T, \mu)$-plane. Note that for $\mu \neq 0$, $\langle\bar{\psi}\psi\rangle_\varphi$ developes an imaginary part, which will be discussed below. A typical example for the behavior of the real part of the $\varphi$-dependent quark condensate at a moderate value of $\mu$ is shown in Fig. 3. At $\varphi = \pi$ we observe the chiral cross-over with temperature indicated by the ordinary quark condensate. At $\varphi = 0, 2\pi$ the condensate rises with temperature similar to $\mu = 0$ as discussed in Ref. [12]. The deconfinement transition is observed along the $\varphi$-direction, when the constant behavior of $\langle\bar{\psi}\psi\rangle_\varphi$ below $T_c$ changes into the typical variations observed above $T_c$ [12]. The new element at finite $\mu$ is the behavior for even larger values of $T$: There $\langle\bar{\psi}\psi\rangle_\varphi$ develops an additional discontinuous structure along the $\varphi$-direction. We have checked that this structure is genuine wrt. variations of our vertex ansatz. For increased chemical potential the temperature where this discontinuity opens moves closer to the deconfinement transition temperature. This suggests that the deconfinement transition may turn from crossover to second or first order at chemical potentials as large as the one of the chiral critical endpoint (see below). Within the accuracy of our numerical calculations we could, however, not yet resolve this issue in detail. This will be addressed in future work. The imaginary part of $\langle\bar{\psi}\psi\rangle_\varphi$, not shown in the figure, is antisymmetric wrt. to $\varphi \to 2\pi - \varphi$. Therefore $\Sigma_{\pm 1} = \int_\varphi \left\{ Re\langle\bar{\psi}\psi\rangle_\varphi \cos(\varphi) \pm Im\langle\bar{\psi}\psi\rangle_\varphi \sin(\varphi) \right\}$ stays real and the difference between quark and anti-quark loops is generated by $Im\langle\bar{\psi}\psi\rangle_\varphi$.

In Fig. 4, we display the main result of this work: the phase diagram of two-flavour QCD. We find a chiral crossover at small chemical potential. The deconfinement crossover happens at somewhat larger temperatures and one observes a characteristic (albeit small) splitting of the transition temperatures from the Polyakov-loop and

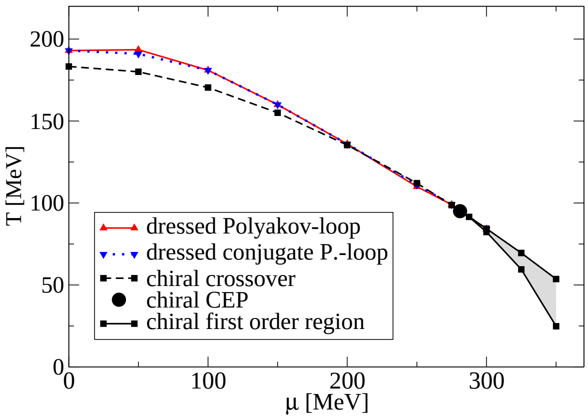


FIG. 4: The phase diagram for chiral symmetry breaking ($\chi$) and deconfinement of quarks ($\Sigma_1$) and anti-quarks ($\Sigma_{-1}$).

its conjugate [7]. At larger chemical potential all transitions come together again. The chiral crossover line goes over into a critical point at approximately $(T_{EP}, \mu_{EP}) \approx (95, 280)$ MeV, followed by the coexistence region of a first order transition. Thus we find the comparatively large value $\mu_{EP}/T_{EP} \approx 3$. We have checked, that these values are not overly sensitive to the details of our truncation: when changing the parameters in the vertex ansatz within a reasonable range we observe variations of $(T_{EP}, \mu_{EP})$ of the order of ten percent. Thus a firm conclusion of the present approach seems to be that $\mu_{EP}/T_{EP} \gg 1$: If there is a critical endpoint, it happens at large chemical potential. This statement agrees with the result of corresponding calculations in the PQM model, once quantum corrections have been taken into account [7]. Expectations from recent lattice calculations at $N_f = 2 + 1$ close to the continuum limit also seem to point in this direction [8].

Certainly, at such large values of the chemical potential, our truncation scheme may no longer be reliable: baryon effects that are not implicitly included in our truncation of the quark-gluon interaction may play an important role here. Also the formation of inhomogeneous chiral condensates may be favored upon the homogeneous one studied here. We believe that our work provides a suitable basis for further investigations in these directions.

**Acknowledgements**
We thank Daniel Mueller and Jan Pawlowski for discussions. This work has been supported by the Helmholtz Young Investigator Grant VH-NG-332 and the Helmholtz International Center for FAIR within the LOEWE program of the State of Hesse.


[1] P. de Forcrand and O. Philipsen, PoS **LATTICE2008** (2008) 208.
[2] L. McLerran, R. D. Pisarski, Nucl. Phys. **A796** (2007) 83-100.
[3] T. Kojo, Y. Hidaka, L. McLerran *et al.*, Nucl. Phys. **A843** (2010) 37-58.
[4] D. Nickel, Phys. Rev. Lett. **103** (2009) 072301.
[5] K. Fukushima, Phys. Lett. **B591** (2004) 277-284. C. Ratti, M. A. Thaler, W. Weise, Phys. Rev. **D73** (2006) 014019.
[6] B. -J. Schaefer, J. M. Pawlowski, J. Wambach, Phys. Rev. **D76** (2007) 074023.
[7] T. K. Herbst, J. M. Pawlowski, B. -J. Schaefer, Phys. Lett. **B696** (2011) 58-67.
[8] G. Endrodi, Z. Fodor, S. D. Katz, K. K. Szabo, [arXiv:1102.1356 [hep-lat]].
[9] Z. Fodor and S. D. Katz, JHEP **0203**, 014 (2002); S. Ejiri, *et al.* Prog. Theor. Phys. Suppl. **153**, 118 (2004); R. V. Gavai and S. Gupta, Phys. Rev. D **71**, 114014 (2005);
[10] C. D. Roberts, S. M. Schmidt, Prog. Part. Nucl. Phys. **45** (2000) S1-S103.
[11] J. Braun and H. Gies, JHEP **0606** (2006) 024; J. Braun, H. Gies, J. M. Pawlowski, Phys. Lett. **B684** (2010) 262-267. J. Braun, Eur. Phys. J. C **64** (2009) 459.
[12] C. S. Fischer, Phys. Rev. Lett. **103** (2009) 052003; C. S. Fischer, J. A. Mueller, Phys. Rev. **D80** (2009) 074029.
[13] C. S. Fischer, A. Maas and J. A. Muller, Eur. Phys. J. C **68** (2010) 165.
[14] J. Braun, L. M. Haas, F. Marhauser, J. M. Pawlowski, Phys. Rev. Lett. **106** (2011) 022002.
[15] J. A. Mueller, C. S. Fischer, D. Nickel, Eur. Phys. J. **C70** (2010) 1037-1049.
[16] S. -x. Qin *et al.*, [arXiv:1011.2876 [nucl-th]].
[17] C. Gattringer, Phys. Rev. Lett. **97** (2006) 032003.
[18] F. Synatschke, A. Wipf and C. Wozar, Phys. Rev. D **75** (2007) 114003;
[19] E. Bilgici, F. Bruckmann, C. Gattringer and C. Hagen, Phys. Rev. D **77** (2008) 094007.
[20] K. Fukushima, Phys. Rev. D **68** (2003) 045004.
[21] A. Cucchieri, A. Maas and T. Mendes, Phys. Rev. D **75** (2007) 076003.
[22] C. S. Fischer and R. Alkofer, Phys. Rev. D **67** (2003) 094020.
[23] D. Nickel, J. Wambach and R. Alkofer, Phys. Rev. D **73** (2006) 114028
[24] C. S. Fischer, R. Williams, Phys. Rev. **D78** (2008) 074006. [arXiv:0808.3372 [hep-ph]].
[25] F. Karsch, E. Laermann, A. Peikert, Nucl. Phys. **B605** (2001) 579-599; A. Ali Khan *et al.* [ CP-PACS ], Phys. Rev. **D63** (2001) 034502; F. Burger, E. -M. Ilgenfritz, M. Kirchner, M. P. Lombardo, M. Muller-Preussker, O. Philipsen, C. Urbach, L. Zeidlewicz, [arXiv:1102.4530 [hep-lat]].